



I S A V

**Journal of Theoretical and Applied  
Vibration and Acoustics**

journal homepage: <http://tava.isav.ir>



## **Experimental study on the impact of variations in the friction material properties on the vibration behaviour of brake pads**

**Mohammad Ravanbod<sup>a</sup>, Salman Ebrahimi-Nejad<sup>\*b</sup>**

<sup>a</sup>*Automotive Research Centre, Department of Mechanical and Energy Systems Engineering, University of Bradford, Bradford, UK*

<sup>b</sup>*Assistant Professor, School of Automotive Engineering, Iran University of Science & Technology, Tehran, Iran*

### **ARTICLE INFO**

*Article history:*

Received 19 August 2023

Received in revised form  
5 October 2023

Accepted 6 November 2023

Available online 26 November 2023

*Keywords:*

Friction Material Properties,

NVH,

Brake Pads,

Finite Element Analysis (FEM),

Machine Learning,

Natural Frequency,

Multiple-Features Linear Regression.

### **ABSTRACT**

Brake noise is often caused by the coupling of the natural frequencies of the disc and pad. To prevent this, it is important to control the natural frequencies of these components, hence, the dispersion of natural frequency values is a critical factor in brake noise determination. This paper examines how the brake pad's natural frequencies and mode shapes are affected by its friction material properties, such as Poisson's ratio, Young's modulus, and shear modulus in different directions. Two brake pad designs from Land Rover are modelled and analysed using finite element analysis (FEA) and experimental modal analysis (EMA). A machine learning algorithm based on multiple-features linear regression is used to identify the main friction material parameters and their relationship to the natural frequencies. The results show that increasing the transverse Young's modulus or decreasing the longitudinal Young's modulus, shear modulus, or Poisson's ratio in all directions can increase the natural frequencies. Consequently, the paper suggests that Poisson's ratio and transverse Young's modulus should be considered when selecting friction compounds for brake pads.

© 2023 Iranian Society of Acoustics and Vibration, All rights reserved.

## **1. Introduction**

Brake squeal often occurs due to a combination of natural frequencies. Therefore, the dispersion of natural frequency values is a crucial element in automobile comfortability determination [1]. When the pad and disc natural frequencies are coupled, brake noise occurs [2-7]. As such, it is critical to determine the effects of friction material properties on pad natural frequencies to

\* Corresponding author:

E-mail address: [ebrahiminejad@iust.ac.ir](mailto:ebrahiminejad@iust.ac.ir) (S. Ebrahimi-Nejad)

<http://dx.doi.org/10.22064/tava.2023.2009608.1226>

choose a friction material with natural frequencies that do not coincide with those of the disc in the frequency range where brake squeal is experienced. This procedure will ensure the disc and pad frequencies will not be coupled together within the desired frequency range. Regarding the sustainability issues, although braking noise and vibration only account for a small portion of total braking force, it may cause auditory discomfort to car drivers due to generating high sound pressure rates [8, 9]. Generally, brake noise occurs in the range of 1-16 kHz [10, 11].

Among all the parts of a brake system, brake pads possess the most critical role. The brake efficiency is significantly dependent on the quality and appropriate composition of the brake pads [12]. Many researchers have attempted to create new friction material formulations by changing the elements or weight percentage to improve their mechanical, chemical, and physical properties [13-16]. The selection of fitting friction material with the required compositions can be made using an experience-based or trial/error approach to creating a novel formulation [17]. In addition, the braking noise highly depends on the brake pad material [18, 19]. There have been many studies on the correlation between friction material properties and braking noise. Kharate and Chaudhari [20] examined the relationship between friction materials and disc brake noise. Using the finite element analysis (FEA) in conjunction with the free-free boundary conditions revealed that, regarding the number of modes and disc stiffness, increasing the ratio of Young's modulus over density results in higher disc natural frequencies of vibration. Nouby et al. [21] considered a variety of materials used in disc brake ingredients. The study found that using an aluminium alloy brake rotor (Al-MMC) and a cast iron calliper, along with friction compounds having Young's modulus of 2.6 GPa, could effectively decrease braking noise. Fieldhouse et al. [22] pointed out that the cause for a noisy brake can be found as much in basic mechanical design as insufficient material selection. Also, Nouby et al. [23] carried out an experimental and numerical study, simultaneously on the disc-brake system. They concluded that an increased Young's modulus of the backplate, or an improved shape of the friction material with chamfers and slots, could minimize braking noise. Belhocine and Ghazaly [24] focused on the relationship between Young's modulus and the stability of a disc-brake system. The results concluded that a higher Young's modulus in the friction material, rotor, backplate, and anchor bracket lessens the unstable frequencies and improves total system performance. Kumar and Kumaran [13] gathered information on friction material formulations and the material features that impact brake performance.

This paper mainly investigates how the brake pad's natural frequencies and vibration modes depend on its material properties, such as Young's modulus, Poisson's ratio, and shear modulus. To do this, a finite element (FE) model of the brake pad was developed and verified by comparing it with experimental modal analysis (EMA) data. The paper also explores how the structural aspect ratios of the brake pad affect the results. The parametric analysis was performed on the acquired data to explore the relationships between the variation of friction properties and the natural frequencies using machine learning (ML). This study may offer some useful insights for choosing suitable friction materials to avoid resonance problems between the brake pad and other brake components.

## **2. Model design**

Two different pad models are studied to assess the influence of structural aspect ratios and pad design on the natural frequency and mode shapes and their relationship to material parameters.

CATIA V5 software is utilized to develop a 3D FE model for each brake pad shown in Figures 1 and 2, respectively. Each brake pad is designed for use on vehicles with different performance levels. Brake pads are manufactured by Land Rover, where Pad-A is called (L405 19"), and Pad-B is called (LR156926), as illustrated in Figure 3. Pad-A is mounted in vehicles that require low brake performance with a small disc diameter, whereas Pad-B has larger aspect ratios and is used in heavy-duty vehicles. The fundamental geometric dimensions of selected brake pads are provided in Table 1.

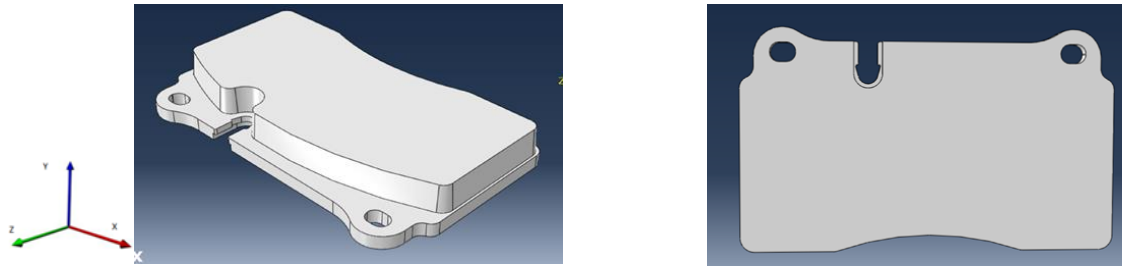


Fig. (1) The 3D model of assembled brake pad-A in different schematic views.

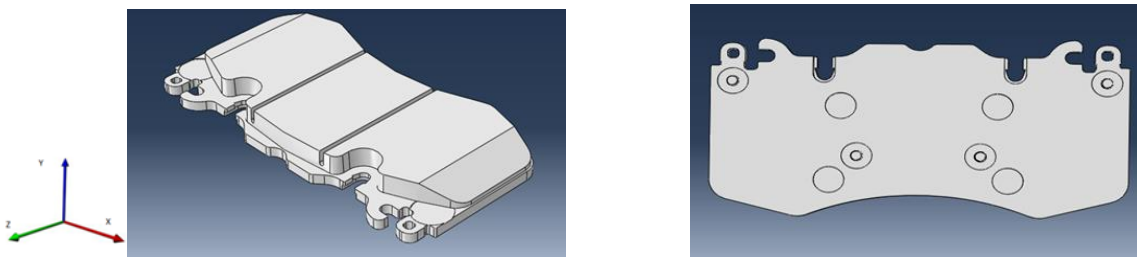


Fig. (2) The 3D model of assembled brake pad-B in different schematic views.



Fig. (3) Illustration of manufactured brake pads. (a) Pad-A. (b) Pad-B.

**Table. (1)** Geometric dimensions of the utilized brake pads.

| Parameters          | Values (mm) for Pad-A | Values (mm) for Pad-B |
|---------------------|-----------------------|-----------------------|
| Length              | 194.42                | 220                   |
| Width               | 105                   | 110                   |
| Friction thickness  | 10                    | 10                    |
| Backplate thickness | 8                     | 8                     |

### 3. Parametric studies

This section will analyse the natural frequency and vibration modes as a function of varying friction material parameters, including Young's modulus, Poisson's ratio, and shear modulus. First, the FEA is employed to calculate the natural frequencies and mode shapes. Then, the EMA is performed to evaluate and validate the FEA outcomes. Finally, the factorial analysis is applied to the results to determine the impact of each material element on the natural frequency, using ML.

#### 3.1. Finite Element Modal analysis

The meshed model with its information for each pad can be found in Table 4. The (C3D8) mesh type is used, and the mesh refinement technique (MRT) is applied to the models to find an acceptable mesh size and number of elements, using the finite element method (FEM) through ABAQUS software. Figure 4 illustrates the results of the mesh sensitivity study to find out at what point the mesh quality does not affect the numerical result. It is observed that the natural frequencies of main mode shapes are independent of the number of elements and density of mesh after approximately choosing 700,000 elements.

The selected friction material is a complex composite with a density of 2950 ( $kg/m^3$ ), and its properties are acquired through a quasi-static test by Land Rover, as listed in Table 2. In the quasi-static test, the composite material was crushed under axial loads to analyse its mechanical properties, such as Poisson's ratio, Young's modulus, and shear modulus. Land Rover conducted a quasi-static uniaxial tensile test on the friction material using an electric universal testing machine (UTM) with a (0N-2KN) load cell. The lower edge of the specimen was fixed with a clamp while the upper edge moved downwards at a rate of 100 N/min, with a maximum applied load of 2KN. We use the orthotropic friction material to determine whether varying material properties in different planes result in different natural frequencies and vibration modes. Isotropic materials are materials whose properties remain the same when measured in different directions, whereas orthotropic materials have three planes, and their properties depend on the direction they are measured. Therefore, using orthotropic friction materials enables us to monitor the influence of Young's modulus, shear modulus, and Poisson's ratio in different plans. Furthermore, a steel plate with isotropic properties is selected for the backplate, and the properties are listed as detailed in Table 3, which are standard material properties for mild steel. This research aims to determine the natural frequencies of brake pads prior to installing them into the disc brake system. Separating the natural frequencies of the brake pad and disc brake is crucial before assembly in order to avoid coupling and resonance issues. Accordingly, the free-free modal analysis is utilized in the phase of the assembled brake pad to understand how the body is treated during this situation. As a result, each brake pad is analysed considering no

external forces to allow the structure to vibrate freely, so that mode shapes related to each natural frequency can be better visualized [19]. Concerning boundary conditions, all boundaries are set free, and the surface contact is tied between the friction material and the backplate.

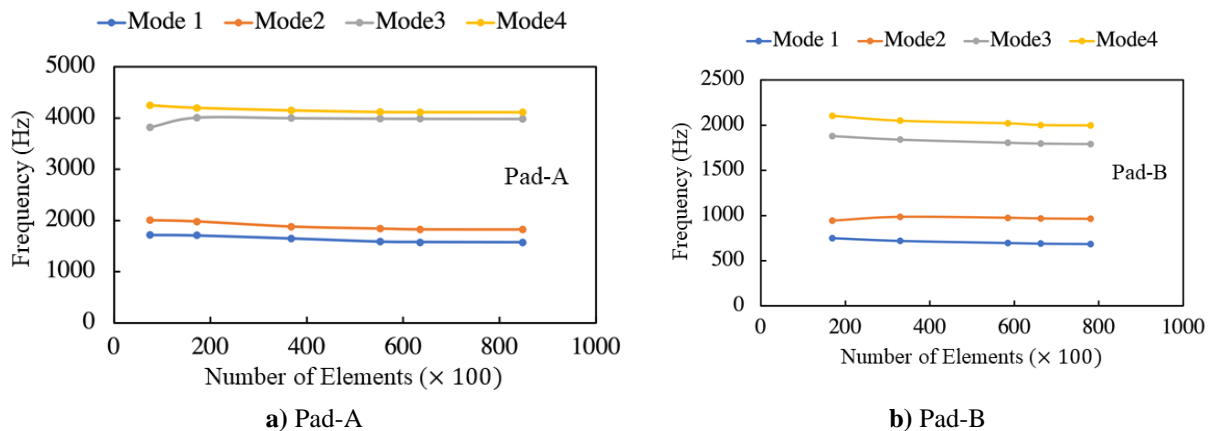
The desired frequency range of the study is selected to be from 1Hz to 20kHz, in which noisy braking typically occurs. In order to study mode shapes, the first four modes are considered as these modes can be significant to squeal. It is not just limited to the first four modes. However, the frequencies of modes beyond the first four modes are potentially too high. Many studies have also shown that focusing on the first four modes is justifiable to reduce both computational and time costs, as the noisy braking mainly happens within the range of the first four modes. By placing various friction material properties, we can study the influence of friction material properties on the main modes of vibration and the pad's natural frequency. Hence, sixteen friction materials were created analytically by varying the properties in ABAQUS software. (Poisson's ratio in the longitudinal plane and the density remain constant).

**Table. (2)** Composite friction material characteristics.

| Density (kg/m <sup>3</sup> ) | Young's modulus (GPa) |     |     | Poisson's ratio |      |      | Shear modulus (GPa) |       |       |
|------------------------------|-----------------------|-----|-----|-----------------|------|------|---------------------|-------|-------|
|                              | E1                    | E2  | E3  | Nu12            | Nu13 | Nu23 | G12                 | G13   | G23   |
| 2950                         | 2.0                   | 2.2 | 2.0 | 0.18            | 0.13 | 0.18 | 0.847               | 0.885 | 0.847 |

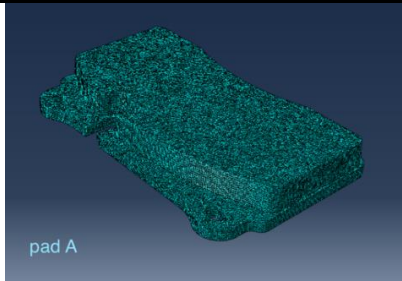
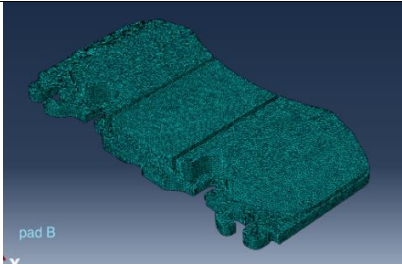
**Table. (3)** Material specification of the backplate.

| Density (kg/m <sup>3</sup> ) | Young's modulus (GPa) | Poisson's ratio |
|------------------------------|-----------------------|-----------------|
| 7800                         | 206.8                 | 0.29            |



**Fig. (4)** Mesh convergence plots for a) pad A, and b) pad B.

**Table. (4)** Specification of the mesh model created for each pad.

| Brake Pad Components   | No. of Elements | Type of Mesh |
|--|-----------------|--------------|
|  <p>pad A</p> | 848105          | C3C8         |
|  <p>pad B</p> | 780373          | C3C8         |

### 3.2. Experimental Modal Analysis

This section evaluates the accuracy of the numerical analysis and ensures that the FEA results are in agreement with the EMA outcomes. In addition, the EMA results are used to tune the FEA. As a result, the natural frequencies and vibration modes of the first four modes of Pad-A (L405 19" Brake Pad) are calculated experimentally. The method used to carry out the test is the impact test. The pad is excited by a modal hammer, and the frequencies are measured by a VSA205 accelerometer. The excitation and response signals are transferred to the data acquisition unit which is DEWE-41-T-DSA type. Afterward, the frequency response function (FRF) measurements are recorded by DEWE/FRF software. By analysing the input excitation and output response simultaneously, natural frequencies and mode shapes are derived by the FRF procedure. Figures 5 and 6 display the test procedure and experiment setup, respectively. The friction material used has the same properties as those listed in Table 2. The FRF method is applied to the pad with the free-free boundary condition considering the same conditions used in the FEA. The analysis is performed up to frequencies of 10kHz. Both the roving accelerometer and impact hammer are used to ensure test accuracy. Nine measurement locations are selected on the specimen as shown in Figure 7. Because the friction material plays a key role in mode shapes, the measurement points are located on the friction material surface. The impact hammer hits the front face of the brake pad in the z-direction, where the friction compound is placed. First, the impact hammer is located close to point 1, and the accelerometer is moved from point 1 to point 9, measuring response signals at different points for the case of the roving accelerometer. Then, the impact hammer is moved to nearly point 2 while the accelerometer roves from point 1 to 9. This cycle is repeated until the hammer reaches point 9. Finally, the DEWE/FRF software calculates the complete mode shapes and their corresponding natural frequency, which are exhibited in Figure 11 and Figure 8, respectively.

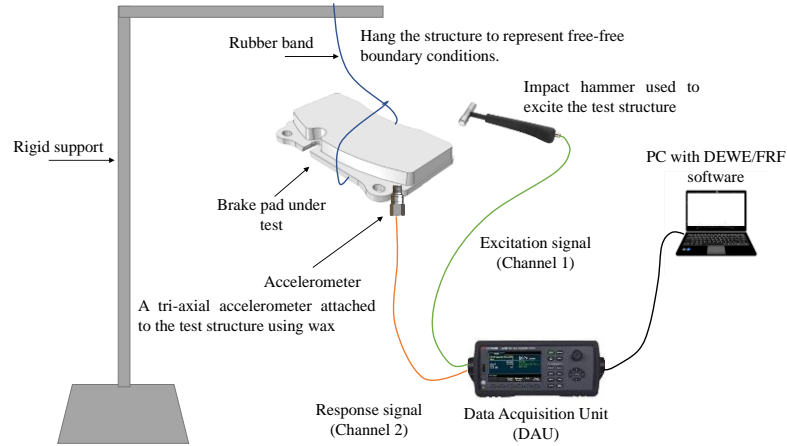


Fig. (5) The schematic diagram of the performed tap-testing.

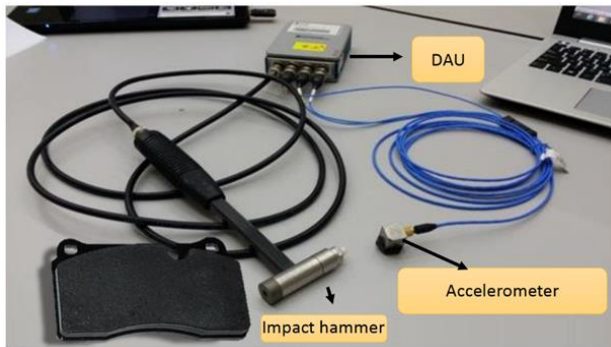


Fig. (6) The EMA implementation.

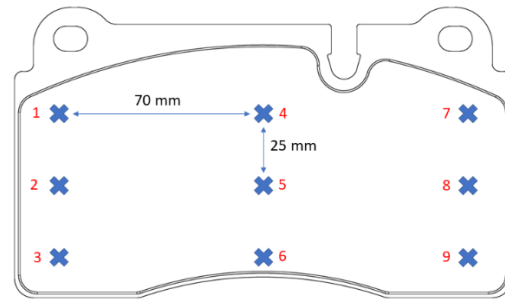


Fig. (7) The location of response measurement and impact excitation points.

### 3.3. Factorial analysis

The fractional factorial analysis is employed to assess the effect of changes in each of the properties on the natural frequency by utilizing Minitab software. Minitab provides us with the capability to run the factorial analysis on the coded properties to determine the most efficacious property on the natural frequency. The multiple-features linear regression algorithm is used to derive the results. Before the parametric analysis starts, properties must be coded based on their maximum and minimum values (using 1 for maximum and -1 for minimum) representing the distance between factor levels and the overall mean to compare them without measuring units. This is beneficial in many ways, such as enabling the comparison and interpretation of parameter estimates, independent of units and scale of the parameters. As the materials are symmetric:

$$E1 = E3 = (E_{X-Y} = E_{Z-Y}) \quad (1)$$

$$Nu12 = Nu23 = (Nu_{X-Y} = Nu_{Z-Y}) \quad (2)$$

$$G12 = G23 = (G_{X-Y} = G_{Z-Y}) \quad (3)$$

so, the selected factors used in the factorial analysis are A = E1, B = E2, C = Nu12, D = G12, and E = G13.

In a full factorial analysis, the total number of runs is determined as a  $(levels)^{(factors)}$ . i.e.  $2^5 = 32$  runs. An alternative to the full factorial is to minimize the number of runs by running a  $(levels)^{(factors-1)}$  fractional factorial design: i.e.  $2^{5-1} = 16$  runs, which is a fraction of the full runs. Due to  $n = 5$  factors being employed in the factorial analysis, sixteen friction materials are needed as sixteen runs are required as shown below:

$$2^{n-1} = \text{The number of runs } (2^{5-1} = 16) \tag{4}$$

The Gradient-descent is used in linear regression for multiple-features and it is assumed that the hypothesis is:

$$h_{\theta} = \theta_0 + \theta_1 x_1 + \theta_2 x_2 + \dots + \theta_n x_n \tag{5}$$

where,  $n = 5$ , and  $\theta_0, \theta_1, \theta_2, \dots, \theta_n$  are regression coefficients, and  $x_1, x_2, \dots, x_n$  are input variables. In addition, the cost function can be calculated as follows:

$$J(\theta) = \frac{1}{2m} \sum_{i=1}^m (h_{\theta}(x)^{(i)} - y^{(i)}) \tag{6}$$

$$\theta = \begin{bmatrix} \theta_0 \\ \theta_1 \\ \theta_2 \\ \theta_3 \\ \theta_4 \\ \theta_5 \end{bmatrix} \tag{7}$$

where  $m$  is the number of training set ( $m = 16$ ), and  $y$  is the output variable in the training set.

It is needed to update the regression coefficients repeatedly until convergence ( $J(\theta)$  reaches near zero and it decreases by less than 0.001 in one iteration). A gradient descent test can be used to verify convergence.

$$\theta_j = \theta_j - \alpha \frac{1}{m} \sum_{i=1}^m (h_{\theta}(x)^{(i)} - y^{(i)}) x_j^{(i)} \tag{8}$$

Computations should simultaneously update  $\theta_j$  for  $j = 0, 1, \dots, n$ .

where  $\alpha$  is the learning rate. As a result, this research allowed us to study the influence of varying Young's modulus, Poisson's ratio, and shear modulus on the natural frequency. The procedure to perform the factorial analysis is as follows: To carry out parametric analysis, we vary the properties of friction materials within certain ranges. These include E1 (1.5GPa-2.5GPa), E2 (2GPa-3GPa), Nu12 (0.1-0.32), G12 (0.06GPa-2.0GPa), and G13 (0.07-2.0GPa). By this, we create 16 different friction material compounds that can be analysed using ABAQUS software. The first four natural frequencies and their corresponding friction properties are calculated and input into Minitab software. Afterwards, the friction variables will be coded using 1, 0, and -1 coding coefficients to make them independent of the units and scale of the parameters. Finally, we run a multiple-feature linear regression algorithm to calculate the objective function and equivalent diagrams.



### 4. Results and discussion

In the following section, the FEA and EMA results are discussed in detail, and the FEA accuracy is validated. Finally, the factorial analysis results are presented, which address the relationship between each property and the natural frequency.

#### 4.1. Natural frequency

Figure 8 depicts the natural frequency against the amplitude ( $g/N$ ) obtained from the FRF measurements. There are amplitude peaks that correspond to each mode's natural frequency. Therefore, the first four peaks represent the first four modes of vibration. Table 5 makes a comparison between the natural frequencies calculated from the FEA and the EMA considering Pad-A. It can be observed that the percentage deviation falls entirely within the acceptable range, and the FEA results are in good agreement with those of the EMA. The deviation fits well within the scope as the maximum deviation is 5.1 percent, which occurs in mode 4. The negligible deviation is caused by composition production variability (variations in geometry and material). The accuracy of FEA has been validated and confirmed by EMA. Consequently, the first four modes of Pad-B have been calculated and their natural frequencies are 685.45Hz, 963.92Hz, 1790.2Hz, and 1997.7Hz, respectively. The mode shapes and their corresponding natural frequencies of Pad-A and Pad-B can be observed in Figure 9 and Figure 10, respectively.

**Table. (5)** The comparison of the natural frequencies calculated by FEA and EMA.

| Type               | Mode 1  | Mode 2  | Mode 3  | Mode 4  |
|--------------------|---------|---------|---------|---------|
| FEM Frequency (Hz) | 1575.2  | 1822.1  | 3985.2  | 4113.7  |
| EMA Frequency (Hz) | 1658.93 | 1764.87 | 4013.88 | 4333.80 |
| Deviation (%)      | 5%      | 3.13%   | 0.71%   | 5.1%    |

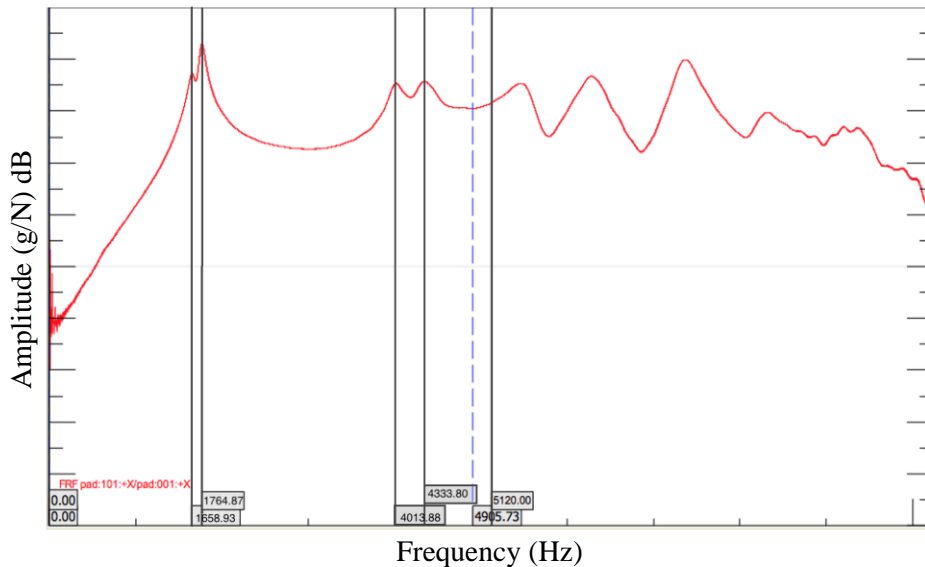


**Fig. (8)** Illustration of the FRF diagram measured for Pad-A.

### 4.2. Mode shapes of vibration

As mentioned earlier, two commercial brake pads were numerically analyzed to derive the natural frequencies and mode shapes. Additionally, Pad-A was subjected to an experimental test to examine the FEA precision. The results indicated that the natural frequencies obtained from the FEA are close enough to those obtained from the EMA. Furthermore, the mode shapes reported by the FEA are identical to those reported by the EMA. The first four modes of vibration derived by the FEA for Pad-A are illustrated in Figure 9, where it can be seen that bending and torsion vibrations have occurred in the first four modes. According to Figure 9 and Figure 11, it is observed that the mode shapes derived by the FEA are the same as those reported by the EMA. Figure 10 presents the mode shapes for Pad-B obtained by the FEA.

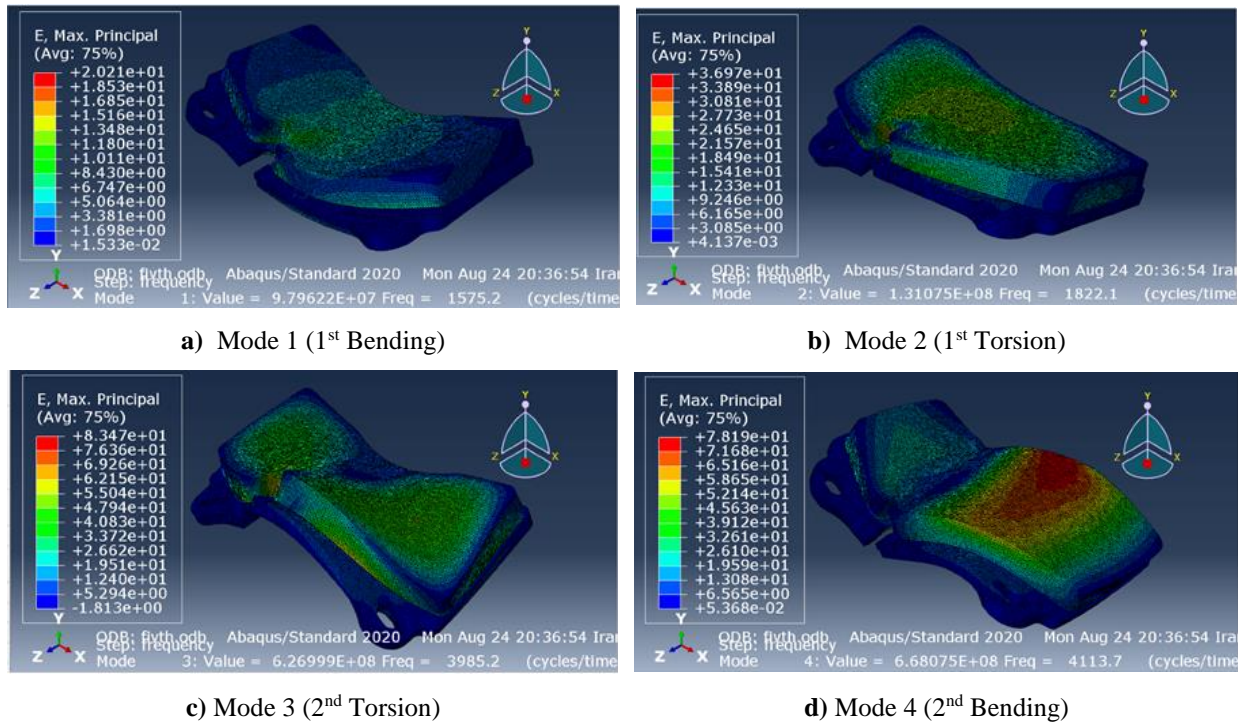


**Fig. (9)** The first four mode shapes correspond to Pad-A.

As seen in Figure 10, bending and torsion mode shapes occurred in the first four modes. The comparison between Figure 9 and Figure 10 shows that the pads exhibit different mode shapes due to their unique designs and aspect ratios. On the other hand, despite changing material properties, the mode shapes for each brake pad remain unchanged, where the FEA demonstrates that all sixteen friction materials have the same first four vibration modes.

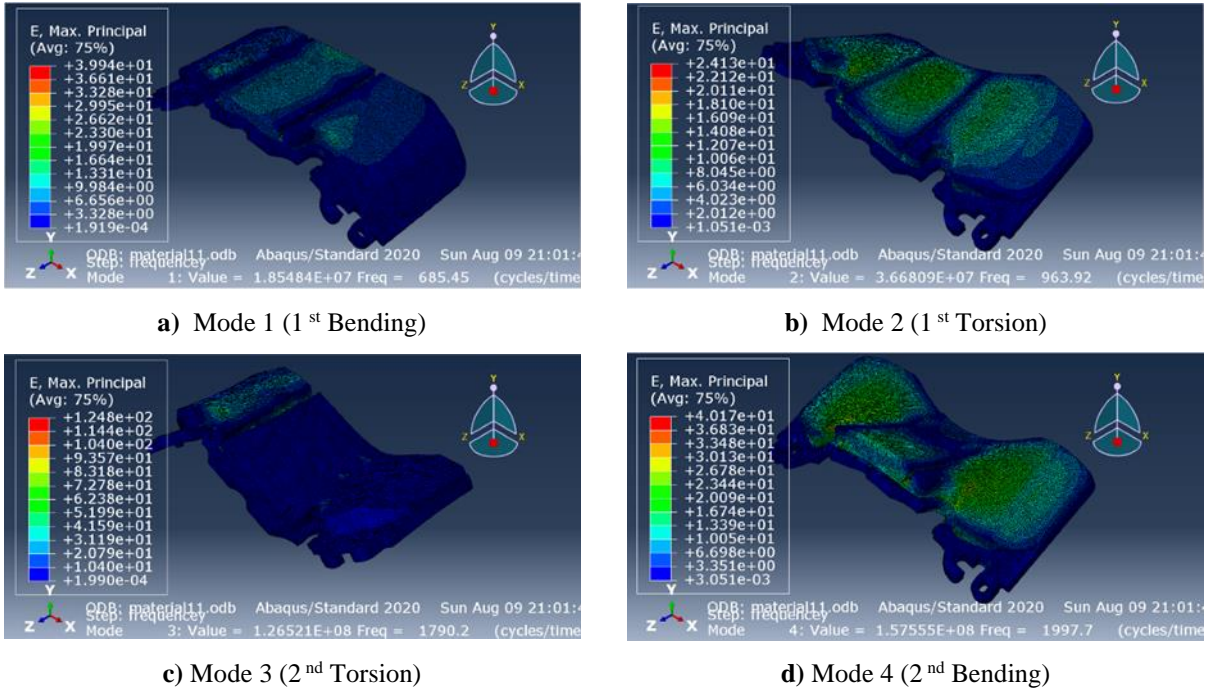


**Fig. (10)** The first four mode shapes correspond to Pad-B.

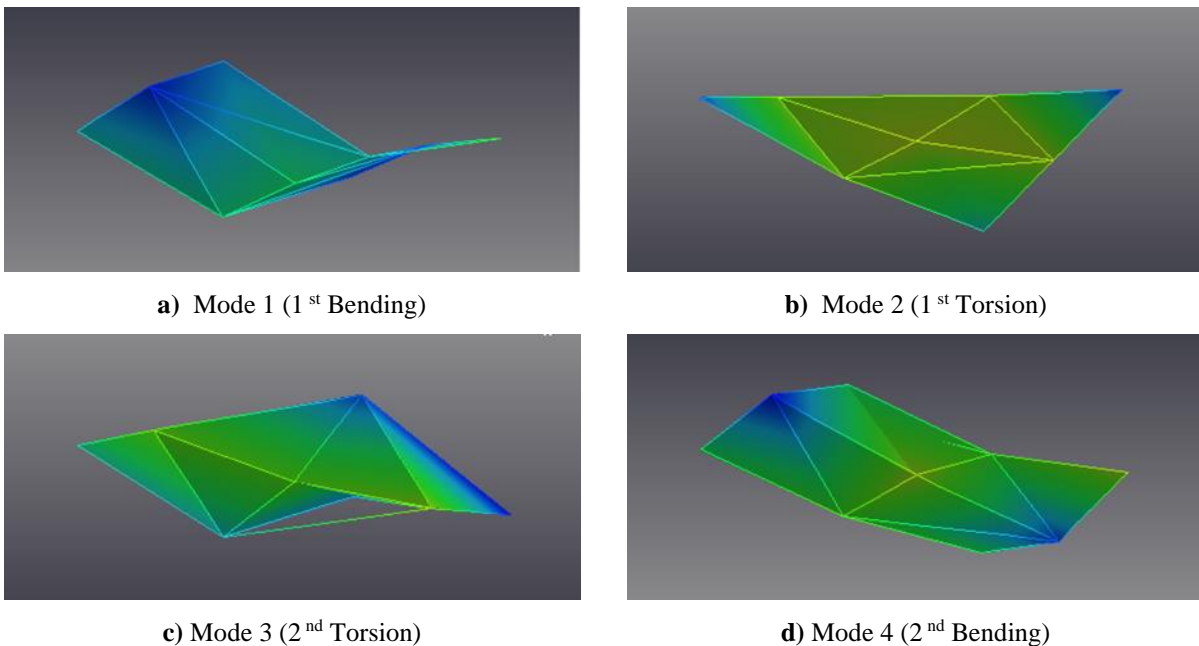


**Fig. (11)** The first four mode shapes correspond to Pad-A obtained from the EMA.

In summary:

- Varying Young's modulus, shear modulus, and Poisson's ratio cannot affect the vibration modes, significantly.
- Aspect ratios greatly influence the vibration modes.

### **4.3. Characteristics effects**

This section presents the results derived from the factorial analysis. According to Figures A1 and A2, the transverse Young's modulus, and Poisson's ratio are the most influential factors on natural frequencies. The results indicate that the natural frequency is more sensitive to the transverse Young's modulus. Also, the natural frequency directly affects the disc-brake system stability [1, 19, 23]. Therefore, the system stability is more dependent on the transverse Young's modulus. The next step is to examine how each property relates to the natural frequency. As illustrated in Figures B1 and B2, it can be concluded that increasing the transverse Young's modulus will result in higher natural frequencies while reducing the longitudinal Young's modulus, shear modulus, and Poisson's ratio in all directions will result in higher natural frequencies. Furthermore, the relationship between the friction characteristics and the natural frequency is valid regardless of pad aspect ratios and geometries and is applicable to any pad.

## **5. Conclusions**

This paper explored how the natural frequencies and mode shapes of the brake pad are influenced by its orthotropic friction material properties, such as transverse and longitudinal Young's modulus, Poisson's ratio, and shear modulus. The present study used the FEM to model and analyse the brake pad and compared the results with the EMA data. The study found that the FEM and EMA results were reasonably consistent in terms of natural frequencies and mode shapes. The study also revealed that the natural frequency dispersion of the brake pad is a critical factor for brake noise prevention, as it can avoid the coupling of the natural frequencies of the brake disc and pad. Therefore, the study suggests that the selection of friction material properties for brake pads should consider their effects on the natural frequency dispersion.

The research findings can be summarized as follows:

- The numerical analysis revealed that the natural frequency increases with the increase of the transverse Young's modulus.
- Conversely, the natural frequency increases with the decrease of the longitudinal Young's modulus, Poisson's ratio, and shear modulus in all directions.
- The transverse Young's modulus has a greater effect on the natural frequency than the other friction material properties.
- The friction material properties (Poisson's ratio, Young's modulus, and shear modulus) do not change the vibration modes of the brake pad.
- The aspect ratios of the brake pad have a significant impact on both the natural frequency and the vibration modes.
- The relationship between the friction characteristics and the natural frequency is valid regardless of pad aspect ratios and geometries and thus applies to any pad.

In future work, the findings of this study can be applied to split the natural frequencies of the brake pad and the disc prior to installation. This can be achieved by selecting a suitable friction

compound that prevents the coupling of their respective natural frequencies. The elimination of this coupling is crucial in reducing disc-brake NVH.

## References

- [1] A. Gallina, W. Lisowski, L. Pichler, A. Stachowski, T. Uhl, Analysis of natural frequency variability of a brake component, *Mechanical systems and signal processing*, 32 (2012) 188-199.
- [2] B. Hervé, J.-J. Sinou, H. Mahé, L. Jezequel, Analysis of squeal noise and mode coupling instabilities including damping and gyroscopic effects, *European Journal of Mechanics-A/Solids*, 27 (2008) 141-160.
- [3] N. Hoffmann, M. Fischer, R. Allgaier, L. Gaul, A minimal model for studying properties of the mode-coupling type instability in friction induced oscillations, *Mechanics research communications*, 29 (2002) 197-205.
- [4] S. Kruse, M. Tiedemann, B. Zeumer, P. Reuss, H. Hetzler, N. Hoffmann, The influence of joints on friction induced vibration in brake squeal, *Journal of Sound and Vibration*, 340 (2015) 239-252.
- [5] A. Lazzari, D. Tonazzi, G. Conidi, C. Malmassari, A. Cerutti, F. Massi, Experimental evaluation of brake pad material propensity to stick-slip and groan noise emission, *Lubricants*, 6 (2018) 107.
- [6] O.I. Abdullah, N. Stojanovic, I. Grujic, The Influence of the Braking Disc Ribs and Applied Material on the Natural Frequency, *International Journal of Precision Engineering and Manufacturing*, (2022) 1-11.
- [7] A. Lazzari, D. Tonazzi, F. Massi, Squeal propensity characterization of brake lining materials through friction noise measurements, *Mechanical Systems and Signal Processing*, 128 (2019) 216-228.
- [8] S.M. Mulani, A. Kumar, H.N.E.A. Shaikh, A. Saurabh, P.K. Singh, P.C. Verma, A review on recent development and challenges in automotive brake pad-disc system, *Materials Today: Proceedings*, 56 (2022) 447-454.
- [9] G. Pan, Z. Liu, Q. Xu, L. Chen, Optimal Design of Brake Disc Structures for Brake Squeal Suppression, in: *Journal of Physics: Conference Series*, IOP Publishing, 2021, pp. 012026.
- [10] N. Kinkaid, O.M. O'Reilly, P. Papadopoulos, Automotive disc brake squeal, *Journal of sound and vibration*, 267 (2003) 105-166.
- [11] A. Lang, An Approach to the solution of disc vibration problems, *Inst. Mech. Engrs.*, 37 (1983) 223-231.
- [12] M.K. Abdelhamid, W. Bray, Braking systems creep groan noise: detection and evaluation, in, *SAE Technical Paper*, 2009.
- [13] V.V. Kumar, S.S. Kumaran, Friction material composite: types of brake friction material formulations and effects of various ingredients on brake performance—a review, *Materials Research Express*, 6 (2019) 082005.
- [14] T. Kato, H. Soutome, Friction material design for brake pads using database, *Tribology transactions*, 44 (2001) 137-141.
- [15] G. Sathyamoorthy, R. Vijay, D. Lenin Singaravelu, Brake friction composite materials: a review on classifications and influences of friction materials in braking performance with characterizations, *Proceedings of the Institution of Mechanical Engineers, Part J: Journal of Engineering Tribology*, 236 (2022) 1674-1706.
- [16] Y. Lu, C.F. Tang, M.A. Wright, Optimization of a commercial brake pad formulation, *Journal of applied polymer science*, 84 (2002) 2498-2504.

- [17] S. Nagesh, C. Siddaraju, S. Prakash, M. Ramesh, Characterization of brake pads by variation in composition of friction materials, *Procedia Materials Science*, 5 (2014) 295-302.
- [18] G. Pan, L. Chen, Impact analysis of brake pad backplate structure and friction lining material on disc-brake noise, *Advances in Materials Science and Engineering*, 2018 (2018).
- [19] S.-m. Lee, J.H. Woo, Y. Cho, D.W. Kim, The Analysis of Brake Squeal Noise Related to the Friction Properties of Brake Friction Materials, in, *SAE Technical Paper*, 2019.
- [20] N. Kharate, S. Chaudhari, Effect of Material Properties On Disc Brake Squeal And Performance Using FEM and EMA Approach, *Materials Today: Proceedings*, 5 (2018) 4986-4994.
- [21] M. Nouby, J. Abdo, D. Mathivanan, K. Srinivasan, Evaluation of disc brake materials for squeal reduction, *Tribology Transactions*, 54 (2011) 644-656.
- [22] J.D. Fieldhouse, W. Steel, A study of brake noise and the influence of the centre of pressure at the disc/pad interface, the coefficient of friction and calliper mounting geometry, *Proceedings of the Institution of Mechanical Engineers, Part D: Journal of Automobile Engineering*, 217 (2003) 957-973.
- [23] M. Nouby, D. Mathivanan, K. Srinivasan, A combined approach of complex eigenvalue analysis and design of experiments (DOE) to study disc brake squeal, *International Journal of Engineering, Science and Technology*, 1 (2009) 254-271.
- [24] A. Belhocine, N.M. Ghazaly, Effects of Young's modulus on disc brake squeal using finite element analysis, *International Journal of Acoustics and Vibration*, 31 (2016) 292-300.

## **Nomenclature**

|                            |                             |
|----------------------------|-----------------------------|
| <b>E</b>                   | Young's modulus             |
| <b>G</b>                   | Shear modulus               |
| <b>Nu</b>                  | Poisson's ratio             |
| <b>g</b>                   | The acceleration of gravity |
| <b>m</b>                   | Number of training sets     |
| <b>n</b>                   | Number of factors           |
| <b>J</b>                   | Cost function               |
| <b>x</b>                   | The input variable          |
| <b>y</b>                   | The output variable         |
| <b><math>\alpha</math></b> | Leaning rate                |
| <b><math>\theta</math></b> | The regression coefficient  |

## **Declaration of competing interest**

There is no known conflict of interest or personal relationship that could have contributed to influencing the research published here.

## **Data access statement**

All data included in this manuscript are available upon request by contacting the corresponding author.

## **Ethics statement**

This material is the authors' own original work, which has not been previously published elsewhere and is not currently being considered for publication elsewhere. The paper reflects the authors' own research and analysis in a truthful and complete manner, and the paper properly credits the meaningful contributions of co-authors and co-researchers.

## **Acknowledgements**

The authors would like to thank Dr David Bryant, the head of the Mechanical Engineering Department at the University of Bradford, for his continuous assistance at the Laboratory of Automotive Engineering.

## **Abbreviations**

|            |                              |
|------------|------------------------------|
| <b>FEA</b> | Finite element analysis      |
| <b>EMA</b> | Experimental modal analysis  |
| <b>FRF</b> | Frequency response functions |
| <b>ML</b>  | Machine learning             |
| <b>MRT</b> | Mesh refinement technique    |

## Appendices

### Appendix A:

#### The effects of material properties on the natural frequency.

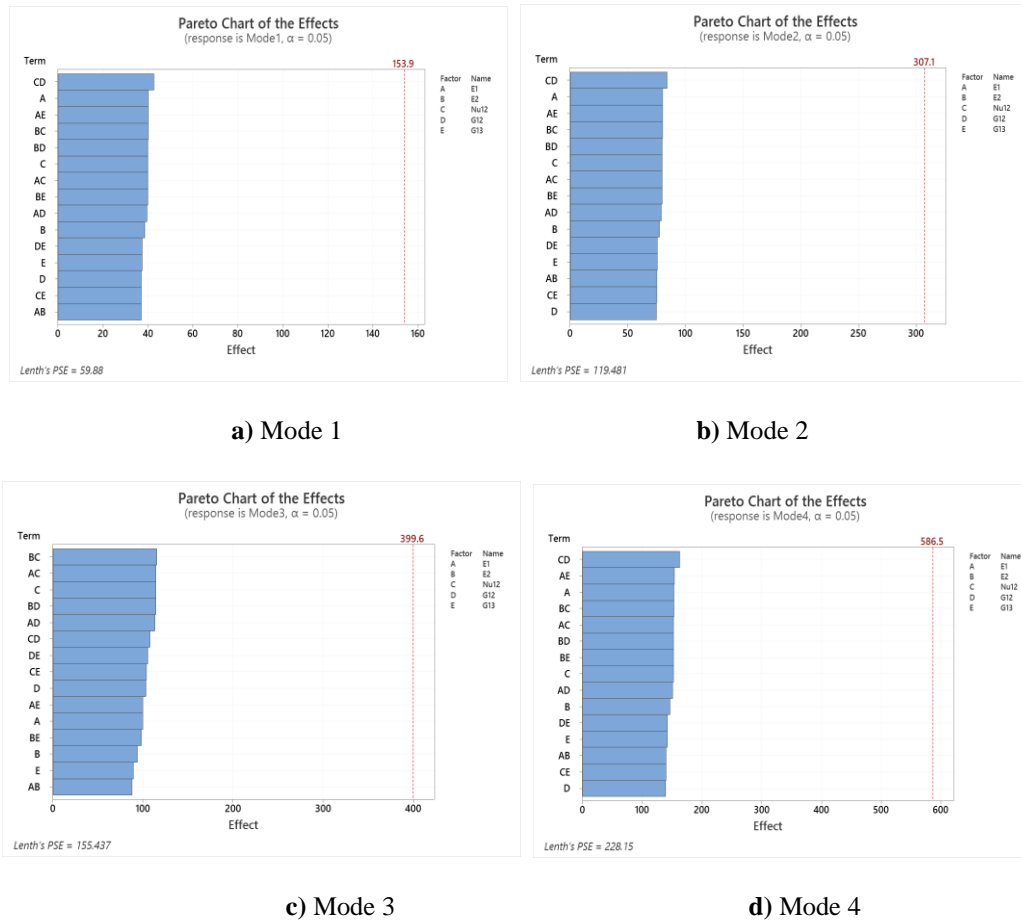
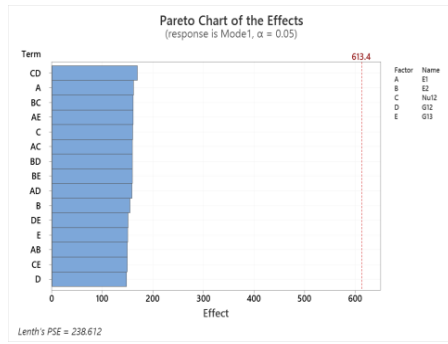
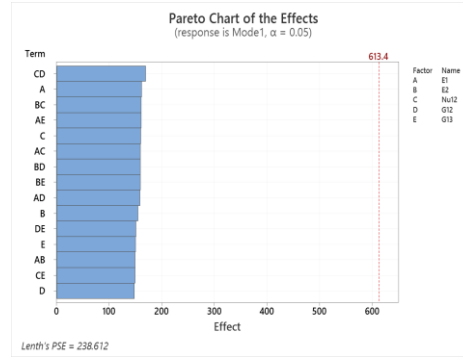


**Fig. (A1)** The impact of friction material factors on the natural frequency of Pad-A

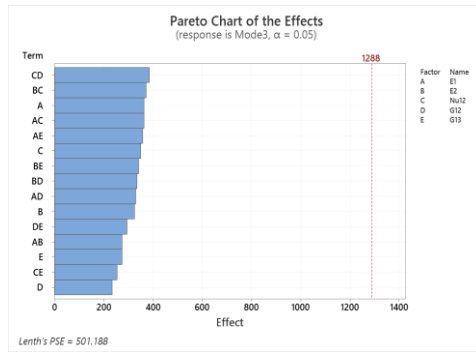




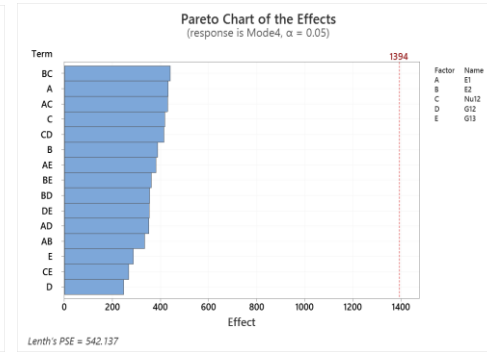
a) Mode 1



b) Mode 2



c) Mode 3



d) Mode 4

Fig. (A2) The impact of friction material factors on the natural frequency of Pad-B

## Appendix B:

### Relationship between material parameters and the natural frequency

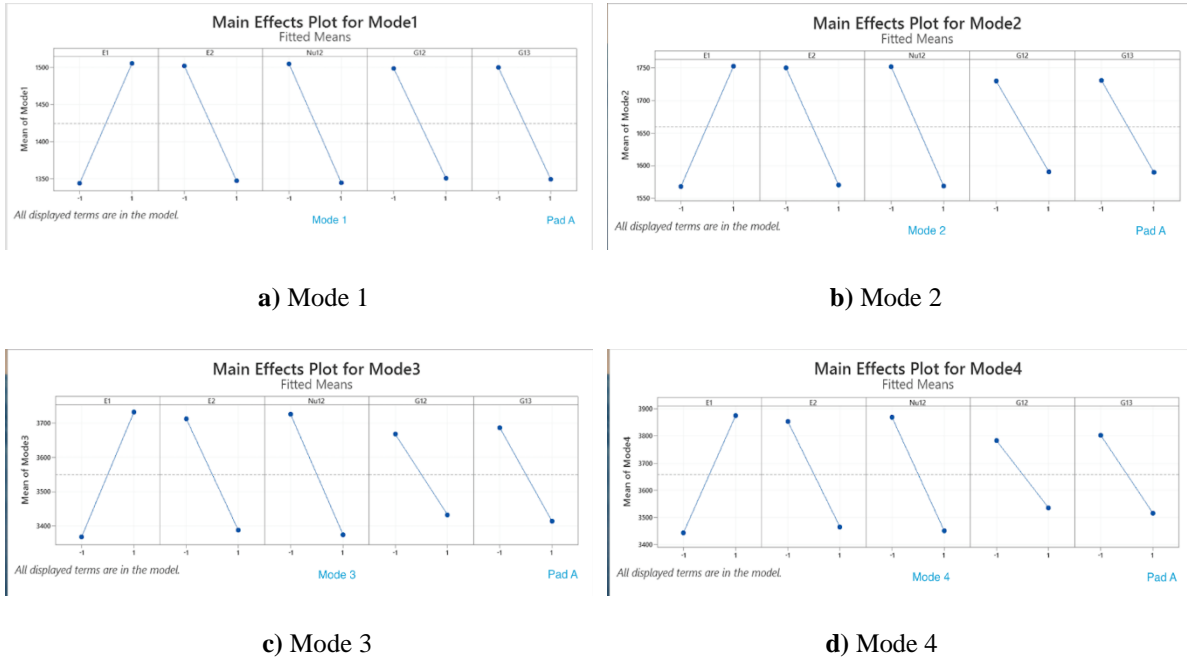


**Fig. (B1)** The relationship between each material parameter and the natural frequency for Pad-A.

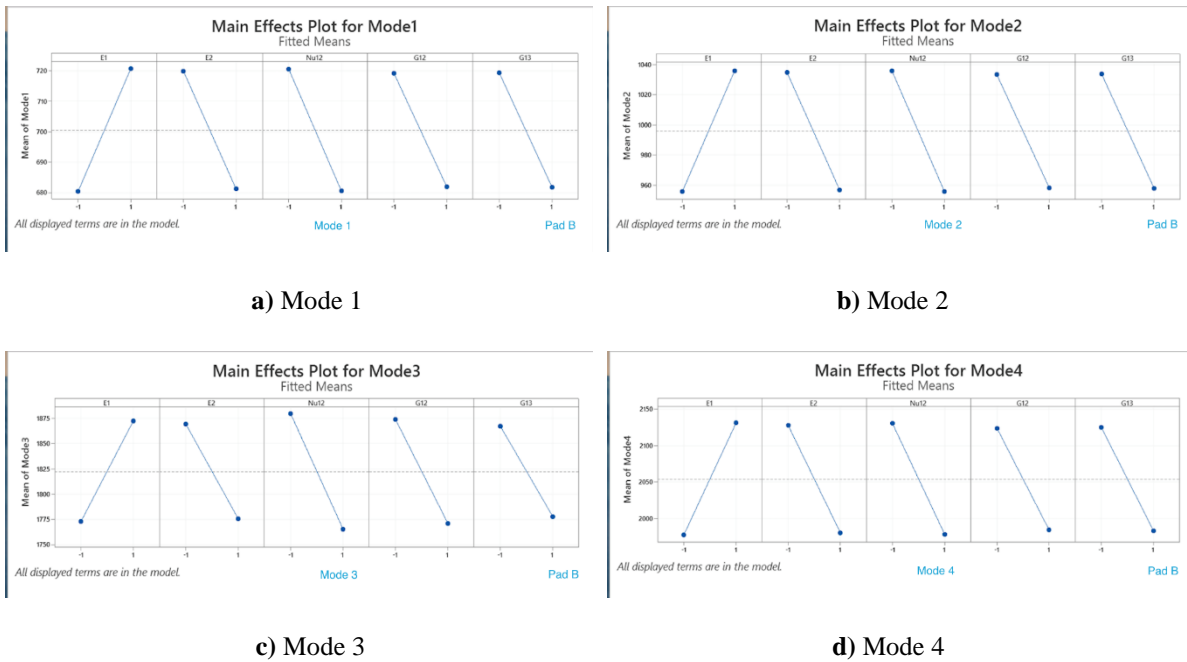


**Fig. (B2)** The relationship between each material parameter and the natural frequency for Pad-B.